

MOL #72504

Batrachotoxin, Pyrethroids and BTG 502 Share Overlapping Binding Sites

On Insect Sodium Channels

Yuzhe Du^{*}, Daniel Garden^{*}, Bhupinder Khambay, Boris S. Zhorov and Ke Dong

Department of Entomology, Genetics and Neuroscience Programs, Michigan State University (Y.D., K.D.), Department of Biochemistry and Biomedical Sciences, McMaster University, Canada (D.G., B.S.Z.) Biological Chemistry Division, Rothamsted Research Ltd, Harpenden, Hertfordshire AL5 2JQ, UK (B.K.), Sechenov Institute of Evolutionary Physiology and Biochemistry, RAS, St. Petersburg, Russia (B.S.Z.)

MOL #72504

Running title: A sodium channel antagonist

Corresponding authors:

Ke Dong, Department of Entomology and Genetics and Neuroscience Programs, Michigan State

University, East Lansing, MI 48824. Tel: 517-432-2034; Fax: 517-353-4354; Email: dongk@msu.edu

Boris S. Zhorov, Department of Biochemistry and Biomedical Sciences, McMaster University, 1280

Main Street West, Hamilton, Ontario, L8N 3Z5, Canada. Tel: 905-525-9140 x 22049; Fax: 905-522-9033;

Email: zhorov@mcmaster.ca

Number of text pages: 16

Number of tables: 1

Number of figures: 5

Number of references: 39

Number of words in the *Abstract*: 253

Number of words in the *Introduction*: 699

Number of words in the *Discussion*: 1,162

ABBREVIATIONS: BTX-B, batrachotoxin; Na_v, Voltage-gated sodium channels; BgNa_v, Cockroach sodium channel; DMSO, dimethyl sulfoxide; MCM, Monte Carlo-minimization. We use a residue-labeling scheme, which is universal for P-loop channels. A residue label includes the domain (repeat) number (1 to 4), segment type (p, P-loop; i, the inner helix; o, the outer helix), and relative position of the residue in the segment (Table 1)

MOL #72504

ABSTRACT

A steroidal alkaloid, batrachotoxin (BTX), and pyrethroid insecticides bind to distinct but allosterically coupled receptor sites on voltage-gated sodium channels and cause persistent channel activation. BTX presumably binds in the inner pore, whereas pyrethroids are predicted to bind at the lipid-exposed cavity formed by the short intracellular linker-helix IIS4-S5 and transmembrane helices IIS5 and IIS6. An alkylamide insecticide BTG 502 reduces sodium currents and antagonizes the action of BTX on cockroach sodium channels, suggesting that it also binds inside the pore. However, a pyrethroid-sensing residue, Phe_{3i17} in IIS6, which does not face the pore, is essential for the activity of BTG 502, but not for BTX. In this study, we found that three additional deltamethrin-sensing residues in IIS6, Ile_{3i12}, Gly_{3i14}, and Phe_{3i16} (the latter two are also BTX-sensing) and three BTX-sensing residues, Ser_{3i15} and Leu_{3i19} in IIS6 and Phe_{4i15} in IVS6, are all critical for BTG 502 action on cockroach sodium channels. Using these data as constraints, we constructed a BTG 502 binding model in which BTG 502 wraps around IIS6 likely making direct contacts with all of the above residues on the opposite faces of the IIS6 helix, except for the putative gating hinge Gly_{3i14}. BTG 502 and its inactive analog DAP 1855 antagonize the action of deltamethrin. The antagonism was eliminated by mutations of Ser_{3i15}, Phe_{3i17}, Leu_{3i19}, and Phe_{4i15}, but not by mutations of Ile_{3i12}, Gly_{3i14}, and Phe_{3i16}. Our analysis revealed a unique mode of action of BTG 502 with its receptor site overlapping with those of both BTX and deltamethrin.

MOL #72504

Introduction

Voltage-gated sodium channels (Na_v) are responsible for the rapid rising phase of action potentials in electrically excitable cells. The pore-forming subunits of Na_v channels contain four homologous repeats, each having six transmembrane helices (S1-S6). Helices S1-S4 form the voltage-sensing domain and transmembrane helices S5 (outer helix) and S6 (inner helix) contribute to the pore-forming domain. The residues connecting the S5 and S6 transmembrane helices form the four reentrant loops, called P-loops. These P-loops contain the amino acid residues, which confer the ion selectivity in Na_v. The voltage sensor is linked to the outer helix S5 by a short extracellular linker helix S4-S5.

Na_v are targets of a diverse natural and synthetic toxins, including therapeutic drugs, insecticides (such as pyrethroids), and naturally occurring toxins (such as batrachotoxin, BTX). Toxins from each group bind to distinct receptor sites on sodium channels and affect channel function (Wang and Wang, 2003). BTX (Fig. 1) isolated from the skin of a Colombian frog (Daly et al., 1965) reduces ion selectivity and causes persistent channel activation by inhibiting inactivation and shifting the voltage-dependence of activation in the hyperpolarizing direction. Pyrethroids, such as deltamethrin (Fig. 1), are synthetic derivatives of the naturally occurring pyrethrum insecticides extracted from *Chrysanthemum* species (Elliott, 1977). Pyrethroids bind to a unique receptor site and inhibit deactivation and inactivation resulting in prolonged opening of sodium channels (Vijverberg and van den Bercken, 1990; Bloomquist, 1996; Narahashi, 2000).

Traditionally, BTX was believed to bind at the lipid-channel interface and alter channel selectivity and gating by an allosteric mechanism (Linford et al., 1998). However, mutational studies identified BTX-sensing residues in the inner helices of all four domains suggesting that BTX is directly exposed to the permeation pathway (Tikhonov and Zhorov, 2005b). More recent mutational and modeling studies have confirmed this prediction (Wang et al., 2006; Wang, et al., 2007a; 2007b; Du et al., 2011a). Studies of the mechanisms of insect resistance to pyrethroids led to the identification of pyrethroid-sensing residues in diverse regions of insect sodium channels (Soderlund, 2005; Davies et al., 2007; Dong, 2007). These data

MOL #72504

have been used to construct a model of the sodium channel where pyrethroids bind to a cavity formed by the linker-helix IIS4-S5, the outer helix IIS5, and the inner helix IIIS6 at the interface between domains II and III (O'Reilly et al., 2006). Systematic site-directed mutagenesis of residues in IIIS6 revealed additional four residues that are important for the action of deltamethrin (Du et al., 2009) and two of them are also critical for the action of BTX (Du et al., 2011a). Despite this apparent overlap, the binding sites for BTX and pyrethroids in IIIS6 are distinct, involving opposite faces of the IIIS6 transmembrane helix (Du et al., 2009).

An alkylamide insecticide BTG 502 (Fig. 1) has been shown to antagonize the binding and action of BTX in ligand-binding and $^{22}\text{Na}^+$ influx assays using mouse brain synaptoneurosomes (Ottea et al., 1989; 1990). These results suggest that BTG 502 and BTX compete for a common receptor site on sodium channels (Ottea et al., 1989). However, unlike BTX, recent data indicate that BTG 502 acts as an antagonist reducing the peak current of insect sodium channels expressed in *Xenopus* oocytes (Du et al., 2011b). Additionally, a residue important for pyrethroid activity, F³¹⁷ in IIIS6, is also critical for the action of BTG 502 (Du et al., 2011b), but not for BTX (Tan et al., 2005). These results suggest that BTG 502 and BTX must have somewhat distinct binding and/or action properties that translate into distinct electrophysiological effects.

Here we conducted mutational analysis and molecular modeling to map the binding site of BTG 502. We found that three additional deltamethrin-sensing residues (two of which are also BTX-sensing) and three BTX-sensing residues are critical for BTG 502 action. Our model incorporates available experimental data on the action of BTG 502 on the cockroach sodium channel BgNa_v and suggests that BTG 502 makes contact with residues on opposite faces of the IIIS6 helix. Therefore, the receptor site for BTG 502 on sodium channels is a unique receptor site that overlaps those of BTX and pyrethroids.

MOL #72504

Materials and Methods

Expression of BgNa_v Sodium Channels in *Xenopus* Oocytes. The procedures for oocyte preparation and cRNA injection are identical to those described previously (Tan et al., 2002). For robust expression of the BgNa_v sodium channels, cRNA was coinjected into oocytes with *Drosophila melanogaster* tipE cRNA (1:1 ratio), which enhances the expression of insect sodium channels in oocytes (Warmke et al., 1997; Feng et al., 1995).

Electrophysiological Recording and Data Analysis. Sodium currents were recorded using standard two-electrode voltage clamping. The borosilicate glass electrodes were filled with filtered 3 M KCl in 0.5% agarose and had a resistance of 0.5 to 1.0 MΩ. The recording solution was ND-96, consisting of 96 mM NaCl, 2.0 mM KCl, 1.0 mM MgCl₂, 1.8 mM CaCl₂, and 10 mM HEPES, pH adjusted to 7.5 with NaOH. Sodium currents were measured with a Warner OC725C oocyte clamp (Warner Instrument, Hamden, CT) and processed with a Digidata 1322A interface (Axon Instruments Inc., Foster City, CA). Data were sampled at 50 kHz and filtered at 2 kHz. Leak currents were corrected by p/4 subtraction. pClamp 9.2 software (Molecular Devices, Sunnyvale, CA) was used for data acquisition and analysis. The maximal peak sodium current was limited to < 2.0 μA to achieve optimal voltage control by adjusting the amount of cRNA injected and the incubation time after injection.

To measure the effect of BTG 502 on the sodium channel, sodium currents were elicited by a 20-ms test pulse to -10 mV from a holding potential of -120 mV after 100 repetitive depolarizing pulses to -10 mV at 10 Hz (Du et al., 2011b). The pyrethroid-induced tail current was recorded during a 100-pulse train of 5-ms depolarization from -120 to 0 mV with a 5-ms interpulse interval. The percentage of channels modified by pyrethroids was calculated using the equation $M = \{[I_{\text{tail}}/(E_h - E_{\text{Na}})]/[I_{\text{Na}}/(E_t - E_{\text{Na}})]\} \times 100$ (Tatebayashi and Narahashi, 1994), where I_{tail} is the maximal tail current amplitude, E_h is the potential to which the membrane is repolarized, E_{Na} is the reversal potential for sodium current determined from the current-voltage curve, I_{Na} is the amplitude of the peak current during depolarization before pyrethroid exposure, and E_t is the potential of step depolarization.

MOL #72504

Data analyses were performed using pClamp 9 (Molecular Devices, Sunnyvale, CA), Origin 8.1 (OriginLab Corp, Northampton, MA) and Adobe Illustrator (Adobe, San Jose, CA) software. Results are reported as mean \pm SD. Statistical significance was determined by using one-way ANOVA with Scheffe's post hoc analysis, and significant values were set at $p < 0.05$ as indicated in the figure legend.

Chemicals. BTG 502 and an inactive analog, DAP 1855 (Fig. 1) were provided by Rothamsted Research Ltd, Harpenden, UK. BTX and deltamethrin were generous gifts from John Daly (National Institutes of Health, Bethesda, MD), and Klaus Naumann and Ralf Nauen (Bayer CropScience AG, Monheim, Germany), respectively. Stock solutions of BTX (1 mM), BTG 502 (50 mM) and deltamethrin (100 mM) were made in dimethyl sulfoxide (DMSO). The working concentration was prepared in ND96 recording solution immediately prior to the experiments. The concentration of DMSO in the final solution was $< 0.5\%$, which had no effect on the function of sodium channels in the experiments. The method for application of chemicals in the recording system was identical to that described previously (Tan et al., 2002). Effects of deltamethrin, BTX, and BTG 502 were measured 10 min after toxin application.

Homology Model of BgNa_v1.1. A homology model of the open cockroach sodium channel variant BgNa_v1-1 was constructed based on the crystal structure of K_v1.2-K_v2.1 chimera channel (Long et al., 2007). Amino acid sequences of the pore domains of BgNa_v1-1 (Fig. 2A) and K_v1.2 were aligned as before (Zhorov and Tikhonov, 2004; Bruhova et al., 2008) and positions of residues are labeled using a universal scheme (Zhorov and Tikhonov, 2004), see Table 1. The extracellular loops, which are too far from residues important for BTX- and deltamethrin activity, were not included in the model. The P-loops were modeled as in (Tikhonov and Zhorov, 2005a). Energy was calculated using the AMBER force field (Weiner et al., 1984; Weiner et al., 1986) and the solvent exposure- and distance dependant dielectric function (Garden and Zhorov, 2010). The atomic charges of the toxin molecules were calculated using the AM1 method (Dewar et al., 1985) through MOPAC. Bond angles were varied in the toxins, but not in the protein. Energy was minimized in the space of generalized coordinates (Zhorov, 1981; Zhorov, 1983). The Monte Carlo-energy minimization (MCM) method (Li and Scheraga, 1987) was used to optimize the channel homology model and to dock the ligands. The SCWRL3 program (Canutescu et al., 2003) was

MOL #72504

used to assign starting conformations of the channel side chains. The ZMM program (www.zmmsoft.com) was used to perform all calculations.

Docking BTG 502. Various binding modes of BTG 502 were explored using distance constraints implied by our experimental data (Supplementary Table S1). A constraint is a flat-bottom parabolic penalty function added to the energy expression. When the distance between a given toxin atom and a given atom in the toxin-sensing residue exceeds the upper limit of the constraint (5 Å in this study), the penalty contribution to the total energy increases sharply, with a force constant of $100 \text{ kcal}\cdot\text{mol}^{-1}\cdot\text{\AA}^{-1}$. The flat-bottom constraint ensures proximity between two atoms, but does not impose specific disposition or orientation of chemical groups the atoms belong to, for instance an H-bond or π -stacking.

To search for the lowest-energy binding modes of BTG 502, we employed our three-stage flexible docking protocol (Garden and Zhorov, 2010). In the first stage, a library of toxin conformers was generated by randomly sampling the toxins torsion angles, followed by energy minimizations to ensure that all the rings were closed. Ten thousand toxin conformations were generated and the ten lowest-energy conformations were collected for docking. In the second stage, the position and orientation of each toxin conformer in the library was sampled 200,000 times by assigning random values to six rigid-body degrees of freedom of the toxin. The energy of the toxin-receptor complexes (including the distance-constraint penalties) was calculated without energy minimization and the ten lowest energy complexes were collected. In the third stage, the ten collected complexes were refined by a 1,000 step MC-minimization and the lowest energy structure was used as the toxin binding model consistent with the given combination of distance constraints. At this stage, the torsion angles in the protein side chains and in the toxin were sampled. Finally, all the distance constraints were removed and the model was MC-minimized to check its intrinsic stability. If during the final MC-minimization the toxin drifted from the constraints-imposed binding mode, the latter was excluded from further analysis.

MOL #72504

Results

Five BTX-sensing residues are critical for the action of BTG 502. We have previously shown that lysine substitutions of two amino acid residues in IIS6, S³ⁱ¹⁵ and L³ⁱ¹⁹ (Fig. 2A, Table S2), dramatically reduce the action of BTX on BgNa_v1-1a channels (Du et al., 2009). Residue F⁴ⁱ¹⁵ in IVS6 (Fig. 2A, Table S2) is important for the binding and action of BTX on mammalian sodium channels (Linford et al., 1998). Here we show that F⁴ⁱ¹⁵ is also a BTX-sensing residue for BgNa_v1-1a channels. BTX (500 nM) inhibited channel inactivation resulting in a noninactivating current and a tail current associated with repolarization of BgNa_v1-1a channels (Fig. 2B). The F⁴ⁱ¹⁵A substitution, which was available from another study (Silver et al., 2009), significantly reduced the action of BTX on BgNa_v1-1a channels (Fig. 2C).

As reported previously (Du et al., 2011b), the effect of BTG 502 on BgNa_v1-1a channels was quite different from those of BTX. In response to 100 repetitive pre-pulses at a frequency of 10 Hz, BTG 502 reduced the amplitude of peak current of the BgNa_v1-1a channel and no tail current was detected upon repolarization (Fig. 2D). To determine whether S³ⁱ¹⁵, L³ⁱ¹⁹ and F⁴ⁱ¹⁵ are also critical for the action of BTG 502, we examined the effect of BTG 502 on the S³ⁱ¹⁵P, S³ⁱ¹⁵K, L³ⁱ¹⁹A, and L³ⁱ¹⁹K mutant channels that were previously made from BgNa_v1-1a channels, as well as the F⁴ⁱ¹⁵A mutant channel. While BTG 502 (10 μM) inhibited 50% of the peak current of the BgNa_v1-1a channel, it only inhibited 23% and 17% for L³ⁱ¹⁹K and F⁴ⁱ¹⁵A mutant channels, respectively (Fig. 2E). Surprisingly, BTG 502 increased the amplitude of peak current of the S³ⁱ¹⁵P and S³ⁱ¹⁵K channels by 5-10%, and 30% for the L³ⁱ¹⁹A channel (Fig. 2E).

Four pyrethroid-sensing residues are critical for the action of BTG 502. Our laboratory recently identified four additional residues in IIS6 (I³ⁱ¹², G³ⁱ¹⁴, F³ⁱ¹⁶, and N³ⁱ²⁰), besides F³ⁱ¹⁷, (Fig. 2A, Table S2) that are critical for the action of pyrethroids (Du et al., 2009). Additionally, we have shown that G³ⁱ¹⁴ and F³ⁱ¹⁶ are also critical for the action of BTX (Du et al., 2011a). To determine whether these residues are also critical for the action of BTG 502, we examined the effect of BTG 502 on these four mutant channels. Substitutions I³ⁱ¹²A, G³ⁱ¹⁴A and F³ⁱ¹⁶A completely abolished the action of BTG 502, while substitution

MOL #72504

N³ⁱ²⁰A did not (Fig. 2F, Table S2). In fact, BTG 502 increased the amplitudes of peak current of I³ⁱ¹²A, G³ⁱ¹⁴A and F³ⁱ¹⁶A channels (Fig. 2F).

BTG 502 and its inactive analog DAP 1855 antagonize the action of deltamethrin. To explore possible interactions between BTG 502 and pyrethroids, we examined the response of the BgNa_v1-1a channel to deltamethrin in the presence of varying concentrations of BTG 502 or DAP 1855. DAP 1855 is an analog of BTG 502 that has no insecticidal activities, but inhibits the binding of BTX to sodium channels in mouse brain synaptoneurosomes (Ottea et al., 1990). With a 100-pulse train of 5-ms step depolarization from -120 to 0 mV at 5-ms intervals, deltamethrin (1 μM) induced a large tail current, as expected for the BgNa_v1-1a channel (Fig. 3A). BTG 502 antagonized the effect of deltamethrin by reducing the amplitude of the tail current in a concentration dependent manner (Fig. 3A). Consistent with the earlier finding (Ottea et al., 1990), DAP 1855 did not affect the peak current of BgNa_v1-1a channels (data not shown), but it antagonized the action of deltamethrin (Fig. 3B).

Amino acid substitution at S³ⁱ¹⁵, F³ⁱ¹⁷, L³ⁱ¹⁹, and F⁴ⁱ¹⁵ abolished BTG 502 antagonism of deltamethrin action. Substitutions S³ⁱ¹⁵P, L³ⁱ¹⁹A, and F⁴ⁱ¹⁵A completely abolished BTG 502 antagonism of deltamethrin action (Fig. 3C, Table S2), whereas substitutions I³ⁱ¹²A, G³ⁱ¹⁴A, F³ⁱ¹⁶A, and N³ⁱ²⁰A did not (Fig. 3D, Table S2). At 10 μM, BTG 502 reduced the activity of deltamethrin on BgNa_v1-1a channels by 50%. Similar levels of antagonism were observed for substitutions I³ⁱ¹²A, G³ⁱ¹⁴A, F³ⁱ¹⁶A and N³ⁱ²⁰A. Because the F³ⁱ¹⁷I and F³ⁱ¹⁷A channels are completely insensitive to pyrethroids and no tail current could be detected (Tan et al., 2005), we used the F³ⁱ¹⁷W channel, which is about 10-fold less resistant to deltamethrin than the F³ⁱ¹⁷A channel, for this experiment. Unlike other pyrethroid-sensing residues in IIIS6, the F³ⁱ¹⁷W mutation abolished the BTG 502 antagonism of deltamethrin activity (Fig. 3D).

Docking BTG 502 in the open channel. Mutational studies show that BTX binds in the inner pore, contacts the inner helices from all four repeats (Wang et al., 2006; Wang et al., 2007a; 2007b), and may adopt an ion-permeable “horseshoe” conformation within the channel as we recently proposed (Du et al., 2011a). In contrast, pyrethroids including deltamethrin are proposed to bind in the lipid-exposed interface

MOL #72504

between the linker-helix IIS4-S5, the outer helix IIS5, and the inner helix IIS6 (O'Reilly et al., 2006; Du et al., 2009). Our data that both BTX-sensing and pyrethroid-sensing residues are critical for the action of BTG 502 indicate that a part of the BTG 502 molecule may bind at the interface between domains II and III, interact with deltamethrin-sensing residues, and also interact with residues that face the inner pore.

We used the above data from our mutational and toxin-binding experiments as distance constraints to dock BTG 502 in the channel model. We explored many combinations of distance constraints (Table S1) and MC-minimized the complex with and then without the distance constraints. The calculations predicted an energetically preferable binding mode, which is most consistent with the experimental data. In this binding mode, BTG 502 wraps around the IIS6 helix (Fig. 4A, B). The amide group of the toxin forms a hydrogen bond with S³ⁱ¹⁵ (Fig. 4C, D). The isopropyl group protrudes into the II/III repeat interface where it interacts with I³ⁱ¹² and F³ⁱ¹⁶. The naphthalene ring also protrudes into the III/IV repeat interface where it interacts with L³ⁱ¹⁹ and forms π -stacking contacts with F³ⁱ¹⁷ and F⁴ⁱ¹⁵ (Fig. 4E). The lipophilic bromine atom faces a hydrophobic site between IIS6 and IIS5. The flexible linker of BTG 502 is exposed to the central pore where it interacts with L³ⁱ¹⁹ (Fig. 4C, D, E). Thus BTG 502 makes direct contacts with all the known BTG 502 sensing residues except the gating-hinge G³ⁱ¹⁴. Using this binding mode we performed further computations to rationalize more experimental observations.

In addition to the BTG 502 binding mode described above, our constraints-driven docking calculations predicted an alternative binding mode in which BTG 502 wraps around IIS6 from the lipid side (not shown). This binding mode appears unlikely as described in legend to Supplementary Figure S1.

Docking BTG 502 in the closed channel. The agonistic effect of BTG 502 when it is applied to sodium channels in combination with scorpion toxin (Ottea et al., 1989) suggests that BTG 502 stabilizes the open conformation of sodium channels. Our data that BTG 502 had no effect without a train of depolarizing prepulses (Du et al., 2011b) indicates preferable binding to open channels. To suggest a possible cause of this state-dependent action, we docked BTG 502 into the KcsA-based homology model of closed BgNa_v1-1 channels. We imposed toxin-channel distance constraints to mimic in the closed channel the BTG 502 binding mode, which we predicted for the open channel. MC-minimizations yielded

MOL #72504

a high-energy complex in which the inner helices were bent at the site where the aromatic ends of BTG 502 protruded into the domain interfaces (Fig. 5 A, B). These results suggested that the channel would not close until the toxin leaves the binding site. Unconstrained MC-minimization of the above complex displaced BTG 502 from the horizontal, IIS6-wrapping mode to a binding mode in which the toxin extended along the pore (Fig. 5 C, D). These calculations suggested that BTG 502 would not bind in the closed channel in the same way as it does in the open channel.

Discussion

BTG 502, an N-alkylamide insecticide, reduces peak sodium currents of the BgNa_v channel and antagonizes the action of BTX (Du et al., 2011b) and deltamethrin, two sodium channel agonists. Using mutational analysis, we found in this study that seven residues in the BgNa_v channel are essential for the action of BTG 502. These are three key BTX-sensing residues, S³ⁱ¹⁵ and L³ⁱ¹⁹ in IIS6 and F⁴ⁱ¹⁵ in IVS6, two deltamethrin-sensing residues I³ⁱ¹² and F³ⁱ¹⁷ in IIS6 and two BTX/deltamethrin-sensing residues, G³ⁱ¹⁴ and F³ⁱ¹⁶ in IIS6. We used these data to create an atomistic model of BTG 502 binding to the BgNa_v channel. In this model, BTG 502 wraps around the transmembrane segment IIS6 and exposes its flexible linker between the bulky ends into the channel pore. This model also shows the interaction of BTG 502 with the pore-facing BTX-sensing residues S³ⁱ¹⁵, L³ⁱ¹⁹ and F⁴ⁱ¹⁵, a deltamethrin-sensing residue I³ⁱ¹², a BTX/deltamethrin-sensing residue F³ⁱ¹⁶ in the II/III interface, and a pyrethroid-sensing residue F³ⁱ¹⁷ in the III/IV interface. Thus, our results delineate a unique receptor site for BTG 502 on the sodium channel and show that the BTG 502 receptor site overlaps with two receptor sites of BTX and deltamethrin.

BTX, veratridine, aconitine and grayanotoxin are classified as site 2 toxins. These toxins share common characteristics in their actions on sodium channels: they bind to the sodium channel in its open state and toxin-modified channels lack fast inactivation and activate at more negative potentials, resulting in persistent channel activation (Wang and Wang, 2003). Studies of the action of BTG 502 on sodium channels in mouse brain synaptoneurosomes using [³H]batrachotoxinin A-20- α -benzoate (BTX-B)

MOL #72504

binding and $^{22}\text{Na}^+$ influx assays (Ottea et al., 1989; 1990) and toxin competition experiments in oocyte-expressed insect sodium channels (Du et al., 2011b) show that BTG 502 antagonizes the action of BTX, suggesting that BTG 502 acts at site 2. However, instead of enhancing channel activation as site 2 neurotoxins do, BTG 502 reduces the amplitude of sodium currents, behaving as an antagonist (Du et al., 2011b). The discovery of BTG 502-sensing residues that are either identical to or distinct from BTX-sensing residues and our model of BTG 502 binding in this study can now explain both common and distinct aspects of the binding and action of BTX and BTG 502. Like BTX, BTG 502 binds to open channels, probably entering from the cytoplasmic side. The agonistic effect of BTG 502 when applied to sodium channels in combination with scorpion toxin (Ottea et al., 1989) suggests that BTG 502 stabilizes the open conformation of sodium channels. Whereas BTX induces persistent activation by providing a hydrophilic path for the permeating ions (Du et al., 2011a), the hydrophobic linker between the naphthalene and alkylamide ends of BTG 502 protrudes in the pore lumen (Fig. 4) thus obscuring the ion conducting path and reducing the amplitude of peak sodium current (Fig. 2D). Interestingly, BTG 502 increased the amplitude of peak current of several mutant channels (Fig. 2E, F). These results suggest that BTG 502 can bind to the F³ⁱ¹⁷A and L³ⁱ¹⁹A mutant channels without obstructing the pore lumen. These mutations could alter the orientation of BTG 502, thus converting it from an antagonist to a weak activator. Further mutational analysis and molecular modeling of BTG 502 with the mutants will be needed to investigate the molecular basis of this agonistic effect.

According to our model, the putative gating-hinge residue G³ⁱ¹⁴ in the middle of IIIS6 is not located within any of the predicted receptor sites for pyrethroids, BTG 502 or BTX. However, it is intriguing that G³ⁱ¹⁴ is critical for actions of three sodium channel toxins, BTG 502 (this study), deltamethrin (Du et al., 2009) and BTX (Du et al., 2011a). Previously we have shown that the G³ⁱ¹⁴A substitution causes a positive shift in the voltage-dependence of activation (Du et al., 2009), indicating an increased stability of the closed state in the mutant channel and that greater depolarization is needed to activate the channel. We speculate that this gating alteration could provide a basis for the observed involvement of G³ⁱ¹⁴ in the

MOL #72504

actions of BTX, deltamethrin, and BTG 502, because all three toxins require open channels for action. The mutation G³ⁱ¹⁴A could alter the positions of other toxin-sensing residues forming a high affinity receptor site. Alternatively, the mutation of the gating hinge may affect the coupling of toxin binding and subsequent gating modifications induced by the toxin.

Our model also provides an explanation for the antagonism of deltamethrin action by BTG 502 and suggests direct competition between the two toxins for their overlapping receptor sites. It appears that occupation of the receptor site of BTG 502 is sufficient for the antagonism of the activity of deltamethrin because DAP 1855, an inactive analog of BTG 502, also antagonized the action of deltamethrin (Fig. 3B). Consistent with this notion, residues S³ⁱ¹⁵, L³ⁱ¹⁹ and F⁴ⁱ¹⁵, which face the pore and contribute to BTX and BTG 502 binding, are all required for BTG 502 to antagonize the deltamethrin action (red symbols in Table S2 and red carbons in Fig. S2), while a pyrethroid-sensing residue N³ⁱ²⁰, which is not required for BTG 502 inhibition, did not alter BTG 502 antagonism of deltamethrin action. However, intriguingly, of the other four pyrethroid-sensing residues, which are critical for BTG 502 inhibition, only F³ⁱ¹⁷ (purple symbols in Table S2 and purple carbons in Fig. S2), but not I³ⁱ¹², G³ⁱ¹⁴ or F³ⁱ¹⁶ (light-blue and green symbols in Table S2 and respectively colored carbons in Fig. S2), is essential for antagonism of deltamethrin action by BTG 502. Our model suggests the following explanation. I³ⁱ¹² and F³ⁱ¹⁶ are in the II/III interface and interact with the isopropyl end of BTG 502 that is extended into the interface. Mutations at these positions would decrease the interactions and the isopropyl end would turn towards the pore axis. Since in the pyrethroid-bound channel, the II/III interface is occupied by the pyrethroid (O'Reilly et al., 2006), the isopropyl group of BTG 502 cannot bind there. The group would turn away from the II/III interface towards the pore. As a result, the antagonistic action of BTG 502 in the deltamethrin-bound channel would be insensitive to the mutations of I³ⁱ¹² and F³ⁱ¹⁶. As far as G³ⁱ¹⁴ is concerned, the alanine mutation of this gating hinge would decrease the open state probability and thus binding of BTG 502 in the open channel. This effect of mutation would be opposed by deltamethrin, a channel activator, explaining why the BTG 502 antagonism is not sensitive to the G³ⁱ¹⁴A mutation.

In summary, using a combination of mutational analyses and computer modeling our study provides

MOL #72504

insights into the molecular action of BTG 502 (a unique partial antagonist) on the sodium channel and its antagonism on the actions of two well-known classes of sodium channel toxins (i.e., BTX and pyrethroids). Our results emphasize the importance of the pore-forming S6 of domain III and its gating hinge in the binding and actions of three distinct classes of sodium channel neurotoxins.

Acknowledgments

We thank Drs. Kris Silver and Eugenio Oliveira for critical review of this manuscript; and Yoshio Nomura, Jung-Eun Lee for making the mutant constructs used in this study.

Authorship Contributions

Participated in research design: Du, Garden, Khambay, Zhorov and Dong.

Conducted experiments: Du and Garden.

Performed data analysis: Du and Garden.

Wrote or contributed to the writing of the manuscript: Du, Garden, Zhorov and Dong.

MOL #72504

References

- Bloomquist JR (1996) Ion channels as targets for insecticides. *Annu Rev Entomol* **41**:163-190.
- Bruhova I, Tikhonov DB and Zhorov BS (2008) Access and binding of local anesthetics in the closed sodium channel. *Mol Pharmacol* **74**(4):1033-1045.
- Canutescu AA, Shelenkov AA and Dunbrack RL, Jr. (2003) A graph-theory algorithm for rapid protein side-chain prediction. *Protein Sci* **12**(9):2001-2014.
- Daly JW, Witkop B, Bommer P and Biemann K (1965) Batrachotoxin. The active principle of the Colombian arrow poison frog, *Phyllobates bicolor*. *J Am Chem Soc* **87**(1):124-126.
- Davies TG, Field LM, Usherwood PN and Williamson MS (2007) DDT, pyrethrins, pyrethroids and insect sodium channels. *IUBMB Life* **59**(3):151-162.
- Dewar MJ, Zebisch EG, Healy EF and Stewart JJ (1985) Development and use of quantum mechanical molecular models. 76. AM1: a new general purpose quantum mechanical molecular model. *J Amer Chem Soc* **107**(13):3902-3909.
- Dong K (2007) Insect sodium channels and insecticide resistance. *Invert Neurosci* **7**(1):17-30.
- Du Y, Garden D, Zhorov BS and Dong K (2011a) Identification of new batrachotoxin-sensing residues in segment IIIS6 of sodium channel. *J Biol Chem* **286**(15):13151-60.
- Du Y, Khambay B and Dong K (2011b) An important role of a pyrethroid sensing residue F1519 in IIIS6 in the action of an alkylamide insecticide BTG 502 on the cockroach sodium channel. *Insect Biochem Molec Biol* **In press**.
- Du Y, Lee JE, Nomura Y, Zhang T, Zhorov BS and Dong K (2009) Identification of a cluster of residues in transmembrane segment 6 of domain III of the cockroach sodium channel essential for the action of pyrethroid insecticides. *The Biochemical journal* **419**(2):377-385.
- Elliott M (1977) *Synthetic pyrethroids*. In *Synthetic Pyrethroids* (ACS Symposium Series No. 42), Washington, DC.
- Feng G, Deák P, Chopra M and Hall LM (1995) Cloning and functional analysis of TipE, a novel membrane protein that enhances *Drosophila para* sodium channel function. *Cell* **82**(6):1001-1011.
- Garden DP and Zhorov BS (2010) Docking flexible ligands in proteins with a solvent exposure- and distance-dependent dielectric function. *J Comput Aided Mol Des* **24**(2):91-105.
- Li Z and Scheraga HA (1987) Monte Carlo-minimization approach to the multiple-minima problem in protein folding. *Proc Natl Acad Sci U S A* **84**(19):6611-6615.
- Linford NJ, Cantrell AR, Qu Y, Scheuer T and Catterall WA (1998) Interaction of batrachotoxin with the local anesthetic receptor site in transmembrane segment IVS6 of the voltage-gated sodium channel. *Proceedings of the National Academy of Sciences of the United States of America* **95**(23):13947-13952.
- Long SB, Tao X, Campbell EB and MacKinnon R (2007) Atomic structure of a voltage-dependent K⁺ channel in a lipid membrane-like environment. *Nature* **450**(7168):376-382.
- Narahashi T (2000) Neuroreceptors and ion channels as the basis for drug action: past, present, and future. *J Pharmacol Exp Ther* **294**(1):1-26.
- O'Reilly AO, Khambay BP, Williamson MS, Field LM, Wallace BA and Davies TG (2006) Modelling insecticide-binding sites in the voltage-gated sodium channel. *The Biochemical journal* **396**(2):255-263.
- Ottea JA, Payne GT, Bloomquist JR and Soderlund DM (1989) Activation of sodium channels and inhibition of [³H]batrachotoxinin A-20- α -benzoate binding by an N-alkylamide neurotoxin. *Molecular pharmacology* **36**(2):280-284.

MOL #72504

- Ottea, JA, Payne, GT, Soderlund, DM, 1990. Action of insecticidal N-alkylamides at site 2 of the voltage-sensitive sodium channel. *J. Agric. Food Chem.* 38, 1724-1728.
- Silver KS, Nomura Y, Salgado VL and Dong K (2009) Role of the sixth transmembrane segment of domain IV of the cockroach sodium channel in the action of sodium channel blocker insecticides. *Neurotoxicology* **30**(4):613-621.
- Soderlund DM (2005) *Sodium channels :Comprehensive Molecular Insect Science*. Elsevier, New York.
- Tan J, Liu Z, Nomura Y, Goldin AL and Dong K (2002) Alternative splicing of an insect sodium channel gene generates pharmacologically distinct sodium channels. *J Neurosci* **22**(13):5300-5309.
- Tan J, Liu Z, Wang R, Huang ZY, Chen AC, Gurevitz M and Dong K (2005) Identification of amino acid residues in the insect sodium channel critical for pyrethroid binding. *Molecular pharmacology* **67**(2):513-522.
- Tatebayashi H and Narahashi T (1994) Differential mechanism of action of the pyrethroid tetramethrin on tetrodotoxin-sensitive and tetrodotoxin-resistant sodium channels. *J Pharmacol Exp Ther* **270**(2):595-603.
- Tikhonov DB and Zhorov BS (2005a) Modeling P-loops domain of sodium channel: homology with potassium channels and interaction with ligands. *Biophys J* **88**(1):184-197.
- Tikhonov DB and Zhorov BS (2005b) Sodium channel activators: model of binding inside the pore and a possible mechanism of action. *FEBS letters* **579**(20):4207-4212.
- Vijverberg HP and van den Bercken J (1990) Neurotoxicological effects and the mode of action of pyrethroid insecticides. *Crit Rev Toxicol* **21**(2):105-126.
- Wang SY, Mitchell J, Tikhonov DB, Zhorov BS and Wang GK (2006) How batrachotoxin modifies the sodium channel permeation pathway: computer modeling and site-directed mutagenesis. *Molecular pharmacology* **69**(3):788-795.
- Wang SY, Tikhonov DB, Mitchell J, Zhorov BS and Wang GK (2007a) Irreversible block of cardiac mutant Na⁺ channels by batrachotoxin. *Channels (Austin, Tex)* **1**(3):179-188.
- Wang SY, Tikhonov DB, Zhorov BS, Mitchell J and Wang GK (2007b) Serine-401 as a batrachotoxin- and local anesthetic-sensing residue in the human cardiac Na⁺ channel. *Pflugers Arch* **454**(2):277-287.
- Wang SY and Wang GK (2003) Voltage-gated sodium channels as primary targets of diverse lipid-soluble neurotoxins. *Cell Signal* **15**(2):151-159.
- Warmke JW, Reenan RA, Wang P, Qian S, Arena JP, Wang J, Wunderler D, Liu K, Kaczorowski GJ, Van der Ploeg LH, Ganetzky B and Cohen CJ (1997) Functional expression of Drosophila para sodium channels. Modulation by the membrane protein TipE and toxin pharmacology. *J Gen Physiol* **110**(2):119-133.
- Weiner SJ, Kollman PA, Case DA, Singh UC, Chio C, Alagona G, Profeta S and Weiner PK (1984) A new force field for molecular mechanical simulation of nucleic acids and proteins. *J Am Chem Soc* **106**:765-784.
- Weiner SJ, Kollman PA, Nguyen DT and Case DA (1986) An All Atom Force-Field for Simulations of Proteins and Nucleic-Acids. *J Comput Chem* **7**(2):230-252.
- Zhorov BS (1981) Vector method for calculating derivatives of energy of atom-atom interactions of complex molecules according to generalized coordinates. *J Struct Chem* **22**:4-8.
- Zhorov BS (1983) Vector method for calculating derivatives of the energy deformation of valence angles and torsion energy of complex molecules according to generalized coordinates. *J Struct Chem* **23**:649-655.

MOL #72504

Zhorov BS and Tikhonov DB (2004) Potassium, sodium, calcium and glutamate-gated channels: pore architecture and ligand action. *J Neurochem* **88**(4):782-799.

MOL #72504

Footnotes

*These authors contributed to the work equally. This study was supported by the National Institutes of Health National Institute of General Medicine [GM057440] and the Natural Sciences and Engineering Research Council of Canada [GRPIN/238773-2009]. Computations were performed using the facilities of the Shared Hierarchical Academic Research Computing Network (SHARCNET: www.sharcnet.ca).

MOL #72504

Legends for figures

Fig. 1. Chemical structures of BTG 502, DAP 1855, batrachotoxin, and deltamethrin.

Fig. 2. Both BTX- and pyrethroid-sensing residues are critical for the action of BTG 502. A, Amino acid sequences of segments IIIS6 and IVS6 in rNa_v1.4 and BgNa_v proteins. BTX-sensing residues S³ⁱ¹⁵, L³ⁱ¹⁹ and F⁴ⁱ¹⁵ are underlined. Pyrethroid-sensing residues I³ⁱ¹², G³ⁱ¹⁴, F³ⁱ¹⁶, F³ⁱ¹⁷ and N³ⁱ²⁰ are in bold. B, Effects of BTX (500 nM) on BgNa_v1-1a channels. C, Substitution F⁴ⁱ¹⁵A reduced the action of BTX on BgNa_v1-1a channels. D, Effects of BTG 502 (10 μM) on BgNa_v1-1a channels. E, Effects of amino acid substitutions for BTX-sensing residues on peak current inhibition by BTG 502. F, Effects of substitutions of pyrethroid-sensing residues on the peak current inhibition by BTG 502 at 10 μM. The peak current reduction by BTG 502 was measured by a 20-ms test pulse to -10 mV from a holding potential of -120 mV following 100 repetitive prepulses to -10 mV at a frequency of 10 Hz before and after the application of 10 μM BTG 502. The asterisks indicate significant differences from the BgNa_v1-1a channel as determined by ANOVA (p<0.05).

Fig. 3. Effects of BTG 502 and DAP 1855 on the action of deltamethrin on BgNa_v1-1a and mutant channels. A and B, Inhibition of deltamethrin-induced tail currents by BTG 502 (A) and DAP 1855 (B). C, Substitutions at the pore-facing positions S³ⁱ¹⁵P, L³ⁱ¹⁹A and F⁴ⁱ¹⁵A abolished BTG 502 antagonism of deltamethrin activity. D, Antagonism of BTG 502 on the action of deltamethrin is abolished by mutation F³ⁱ¹⁷W, but not by alanine substitutions of I³ⁱ¹², G³ⁱ¹⁴, F³ⁱ¹⁶, and N³ⁱ²⁰. Percentage of channel modification by deltamethrin before (solid bar) and after (stripe bar) the application of 10 μM BTG 502 were calculated using the equation $M = \{ [I_{tail}/(E_h - E_{Na})] / [I_{Na}/(E_t - E_{Na})] \} \times 100$. The deltamethrin-induced tail current was recorded after a 100-pulse train of 5-ms step depolarizations from -120 to 0 mV with 5-ms interpulse intervals with a 20 ms test pulse to 0 mV. For the F³ⁱ¹⁶A, F³ⁱ¹⁷W and N³ⁱ²⁰A channels which were 10- to 20-fold more resistant to deltamethrin than the BgNa_v1-1a channel (Tan et al., 2005; Du et al., 2009), 10

MOL #72504

μM of deltamethrin was used. For the I^{312}A channel which was 10-fold more sensitive to deltamethrin than the wild-type (Du et al., 2009), 0.1 μM was used. For the rest of the mutant channels, 1.0 μM was used. The asterisks indicate significant differences after BTG 502 antagonize the action of deltamethrin ($p < 0.05$).

Fig. 4. BTG-502 in the pore domain of BgNav1-1. Repeats I, II, III, and IV are colored brown, gray, green, and blue, respectively. S5s, P-helices, and S6s are shown as thin, intermediate-size, and thick helices, respectively. The ascending limbs are shown as thin C-alpha tracings. The ligand (rendered by sticks with yellow carbons) wraps around IIIS6 and exposes its termini into the II/III and III/IV domain interfaces. Shown are top (A) and the side (B) views and their zoomed images (C and D). Panel E is the top view of the pore domain in which parts of the transmembrane helices at the level of the bound BTG-502 are shown by transparent surfaces. In the proposed binding mode, BTG-502 would partially obstruct the ion permeation by the hydrophobic linker exposed into the pore (A,C, E). The isopropyl group of BTG 502 contacts residues I^{312} and F^{316} , which do not face the pore, while the amide oxygen accepts an H-bond from S^{315} (C). L^{319} is below the hydrophobic linker (D). The naphthalene ring of BTG 502 protrudes in the interface between domains III and IV where it is flanked by F^{317} and F^{415} and forms π -stacking interactions with these residues (C, D).

Fig. 5. The closed-channel KcsA-based models of BgNav1-1 Monte Carlo-minimized with BTG 502. (A and B) Extracellular and side view of the complex obtained with ligand-channel constraints applied to keep BTG 502 in the binding mode, which has been predicted for the open channel (Fig. 4). To accommodate the toxin, the inner-helix IIIS6 (green) has bent significantly as compared to IS6 (orange). Strong toxin-channel repulsions found in the MC-minimized structure (data not shown) indicate that BTG 502 in this binding mode would resist the channel deactivation. (C, D) Top and side views at the complex

MOL #72504

obtained without the channel-toxin constraints. BTG 502 relocated from the starting position (A, B) to the central cavity and adopted a folded conformation.

MOL #72504

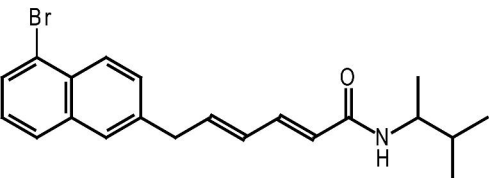
TABLE 1. Sequence alignment

Channel	Domain	First residue #	o1 	o11 	o21 	
KcsA	M1	23	LHWRAAGAAT	VLLVIVLLAG	SYLAVLAER	
K _v 1.2	S5	323	ASMRELGLLI	FFLFIGVILF	SSAVYFAEA	
BgNa _v 1-1	IS5	265	ESVKNLRDVI	ILTMFSLSVF	ALMGLQIYM	
	IIS5	902	RTVGAL <u>G</u> NLT	FV <u>L</u> CIIIFIF	AVMGMQLFG	
	IIIS5	1397	QAIPSIFNVL	LVCLIFWLIF	AIMGVQLFA	
	IVS5	1715	MSLPALFNIC	LLLFLVMFIF	AIFGMSFFM	
			p33 	p41 	p51 	
KcsA	P	59	LITYPRAL	WWSVETATTV	GYGDLYPV	
K _v 1.2	P	358	FPSIPDAF	WWAVVSMTTV	GYGDMVPT	
BgNa _v 1-1	IP	300	CIKNFWAF	LSAFRLMTQD	YWENLYQL	
	IIP	937	VERFPHSF	MIVFRVLCGE	WIESMWDC	
	IIIP	1436	STTLISKAY	LCLFQVATFK	GWIQIMND	
	IVP	1750	GLDDVQSM	ILLFQMSTSA	GWDGVLDG	
			i1 	i11 	i21 	i31
KcsA	M2	86	LWGRLVAVVV	MVAGITSFGL	VTAAATWTFV	GREQERR
K _v 1.2	S6	385	IGGKIVGSLC	AIAGVLTIAL	PVPVIVSNFN	YFYHRET
BgNa _v 1-1	IS6	402	PWHMLFFIVI	IFLGSFYLVN	LILAIVAMSY	DELQKKA
	IIS6	981	WSCIPFFLAT	VVIGNLVVLN	LFLALLLSNF	GSSNLSA
	IIIS6	1506	IYMYLYFVFF	I <u>I</u> <u>F</u> <u>G</u> <u>S</u> <u>F</u> <u>F</u> <u>T</u> <u>L</u> <u>N</u>	LFIGVIIDNF	NEQKKKA
	IVS6	1806	TVGLAFLLSY	LVIS <u>F</u> FLIVIN	MYIAVILENY	SQATEDV

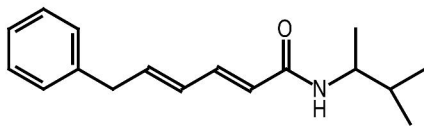
Bold-typed and underlined are experimentally determined residues that, when mutated, affect action of BTG 502 and deltamethrin, respectively.

Position of a residue is designated by a symbol, which identifies a segment, and a relative position of the residue in the segment. Symbols “k”, “o”, “p” and “i”, represent, respectively, the S4-S5linker, the outer helix, the P-loop, and the inner helix.

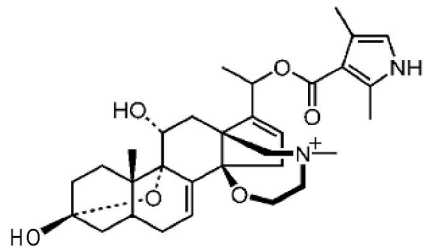
Figure 1



BTG 502



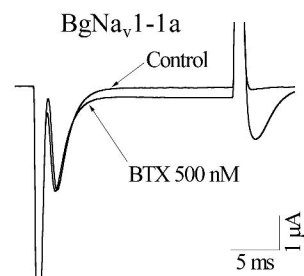
DAP1855



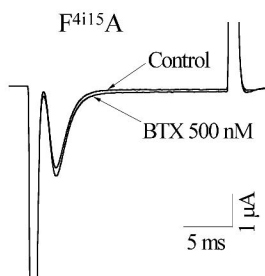
A

IIIS6	rNa_v1.4	MYLYF	VIFII	FGSFF	TLNLF	IGVII	DNF
	BgNa _v 1-1	MYLYF	VFFII	FGSFF	TLNLF	IGVII	DNF
				3i15	3i19		
IVS6	rNa_v1.4	GICFF	CSYII	ISELI	VVNMY	IAIIL	ENF
	BgNa _v 1-1	GIAFL	LSYLV	ISELI	VINMY	IAVIL	ENY
				4i15			

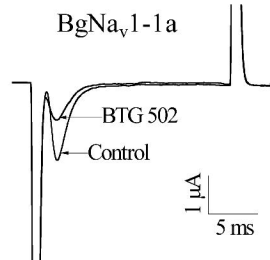
B



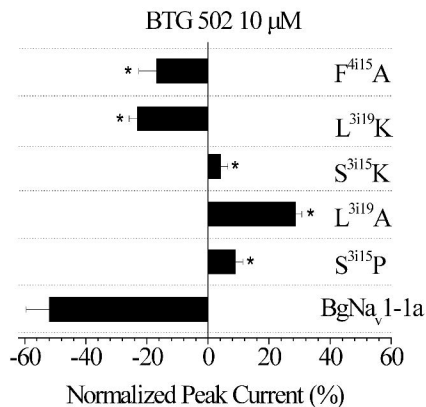
C



D



E



F

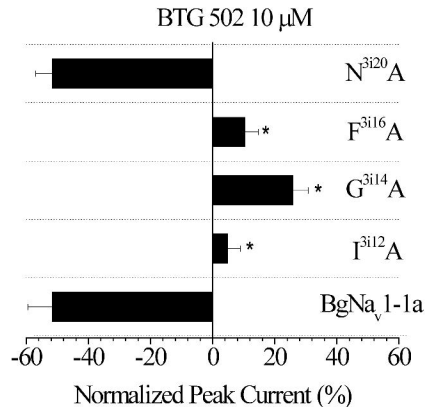
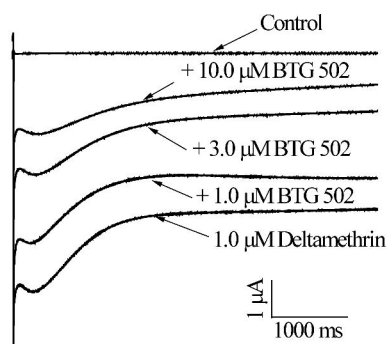
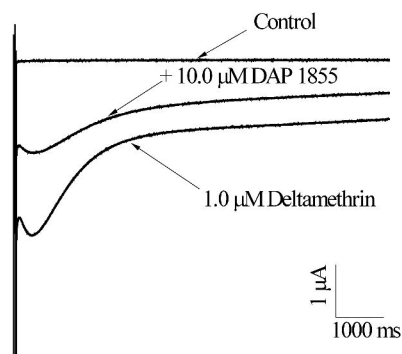


Figure 3

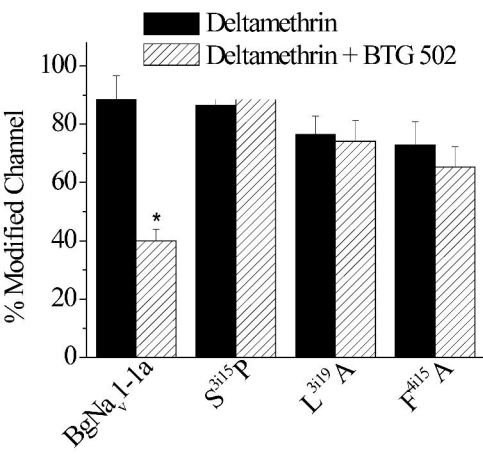
A



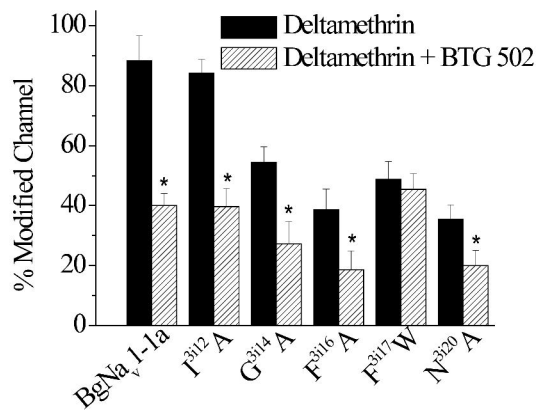
B



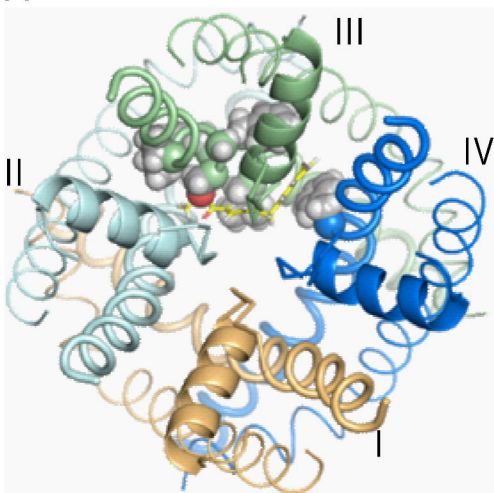
C



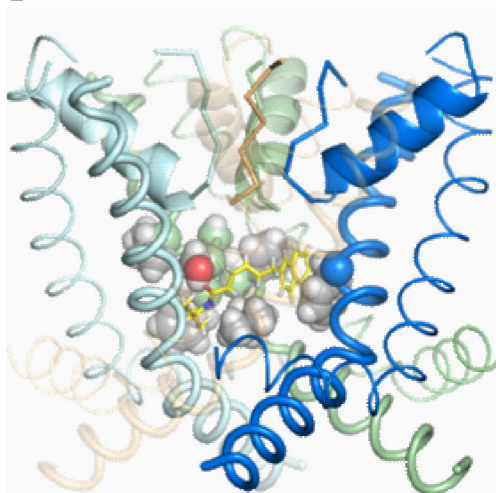
D



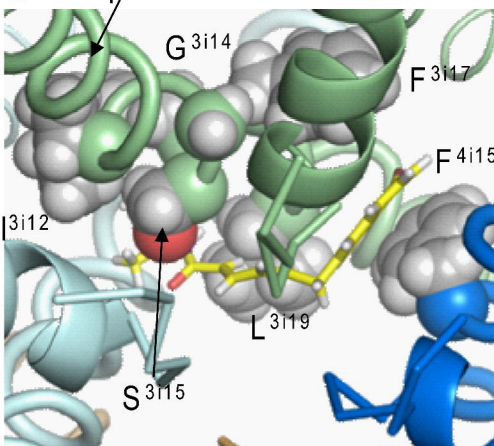
A



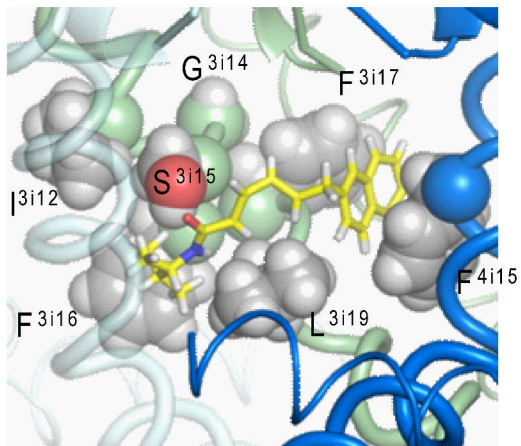
B



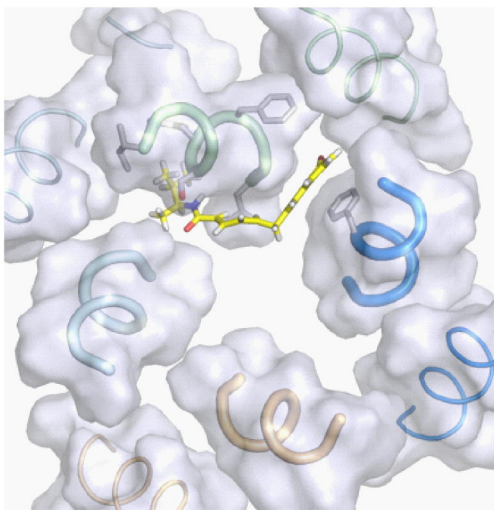
C



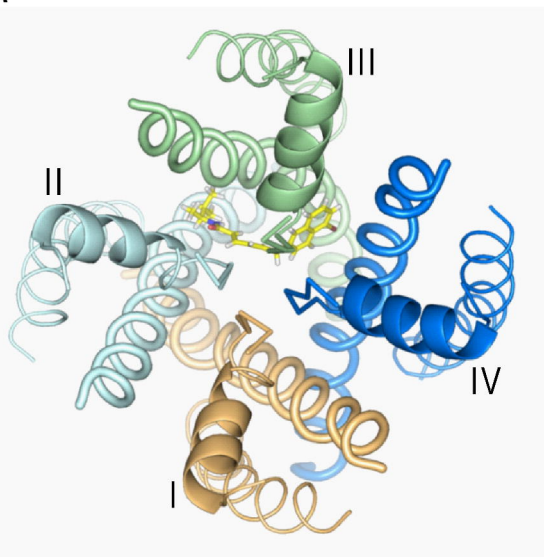
D



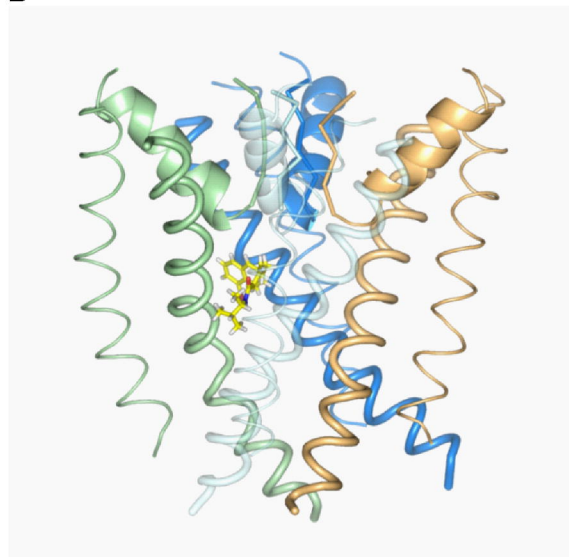
E



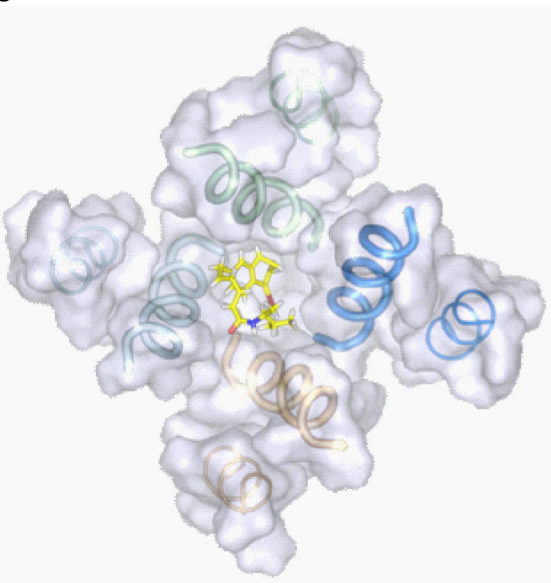
A



B



C



D

